Modeling of the interaction force between the instrument and the trocar in minimally invasive surgery

J. Verspecht, T. Delwiche, A. Buttafuoco, L. Catoire, S. Torfs and M. Kinnaert
Control Engineering and System Analysis Department
Faculty of Applied Science
Université Libre de Bruxelles (U.L.B.)
Brussels, Belgium
corresponding author email: jonathan.verspecht@ulb.ac.be

***Abstract*—Trocars used in Minimally Invasive Surgery (MIS) are equipped with a sealing mechanism. During the motion of an instrument through a trocar, the sealing mechanism deforms itself. None of the friction models presented in the literature capture the macroscopical deformation of the seal mechanism. Therefore a specific hybrid model is developed to describe the movement of an instrument through a trocar. Two operating modes are distinguished, corresponding to the deformation of the sealing mechanism on the one hand, and to the sliding phase through the trocar on the other hand. The model is identified and validated using experimental data recorded on a dedicated test setup.**

I. Introduction

In minimally invasive surgery (MIS), the surgeon performs small incisions ($1cm$) through which long instruments are inserted into the patient body. Besides, for certain operations, gas is injected into the patient body in order to push away the organs and so create a clear operation area. To keep the incisions open and to avoid significant gas leaks, sealing mechanisms called trocars are used.

Understanding and modeling the movement of the instrument through the trocar is important for the development of control laws in teleoperated MIS. Teleoperation consists in performing a remote task with an electromechanical master-slave device. In MIS, the surgeon manipulates a master robot while a slave robot reproduces movement inside the patient body. In order to study force feedback in teleoperated MIS, it is useful to develop a simulator of the teleoperation system interacting with its environment. The work reported here focuses on the movement of the instrument manipulated by the slave robot through a trocar, and more precisely on the interaction force between the instrument and the trocar.

Modeling the forces between two bodies in contact has been the object of a huge number of papers on friction modeling. The friction force depends on many factors, e.g. the relative velocity, the materials, the presence of lubricant. Numerous models exist in the literature, the static friction models (Coulomb model and Stribeck model) and the dynamical models (Dahl Model, LuGre Model, Leuven Model and the Maxwell-Slip model) [1]. The dynamical friction models deal with asperities deformation [2]. Asperities are microscopical irregularities present on every surface. The Maxwell-Slip model has been used as a source of inspiration in our work. However, as the seals used in trocars are subject to large deformation ($\approx 1cm$), the hypothesis of microscopic deformation does not hold. Hence a specific hybrid model has been developed and validated experimentally for our application.

This paper is organized as follow. The Maxwell-Slip Model and the Generalized Maxwell-Slip Model are recalled in section II. The derivation of the new model for the interaction force between the instrument and the trocar is presented in section III. A systematic approach for the identification of the model from experimental data is reported in section IV together with a successful validation of the approach. And finally conclusions are presented in section V

II. Friction Modeling

Two operating modes can be distinguished when analyzing the movement of a medical device into a trocar (see figure 1): the deformation of the seal and the sliding of the instrument through the trocar. A similar distinction is also made in the Maxwell slip model, but under the assumption of microscopic deformation, as recalled in the next section.

A. The Maxwell-Slip Model

The Maxwell-Slip Model (MS model) is based on an assembly of N elementary elasto-sliding elements, called MS-elements. All these MS-elements act in parallel in order to implement the presliding hysteresis behavior of the friction force [3]. The MS-elements share a common input velocity $v(t)$ and each element has its own output force $f_i(t)$ ($i \in \{1, 2, ..., N\}$). Referring to figure 2, the *i*th element is characterized by its internal state z_i (corresponding to the spring deflection) and

The work of Jonathan Verspecht is supported by a FRIA grant. The experimental setup is financed by the FNRS. This paper presents research results of the Belgian Network DYSCO (Dynamical Systems, Control and Optimization) funded by the Interuniversity Attraction Poles Program, initiated by the Belgian State, Science Policy Office. The scientific responsibility rests with its authors.

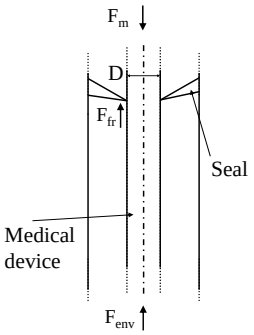

Fig. 1. Schematic of a trocar equipped with a one stage sealing mechanism

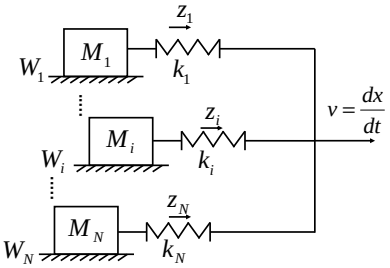

Fig. 2. Schematic of the Maxwell-Slip Model

its stiffness k_i. A MS element is also characterized by a limit force F_i . Each MS elements is described by

$$\dot{z}_i(t) = \begin{cases} v(t) & \text{in sticking mode} \\ 0 & \text{in sliding mode} \end{cases} \quad (1)$$

$$f_i(t) = k_i z_i(t) \quad (2)$$

The *i*th element switches from the sticking mode to the sliding mode when the absolute value of its output force $|f_i(t)|$, computed by equation (2), reaches the limit force F_i. The transition from the sliding to the sticking mode occurs upon a reversal of the input velocity $v(t)$. The total friction force is computed using equation (3) below, where $\beta v(t)$ represents the viscous friction.

$$F_f(t) = \sum_{i=1}^{N} f_i(t) + \beta v(t) \quad (3)$$

The constant limit force F_i is related to a stationary friction behavior of the Coulombian type with viscosity. Indeed if all the MS elements are in sliding state, $|f_i(t)| = F_i \ \forall i \in \{1, 2, ..., N\}$. The output equation (3) becomes:

$$F_f = \sum_{i=1}^{N} F_i sgn(v) + \beta v = F_c sgn(v) + \beta v \quad (4)$$

B. The Generalized Maxwell-Slip Model

The Generalized Maxwell-Slip model (GMS model) [4] is an extension of the Maxwell-Slip model to a velocity dependent sliding force $F_i(v(t))$. In this case the dynamics of each element, called GMS element, is determined by:

$$\dot{z}_i(t) = \begin{cases} v(t) & \text{in sticking mode} \\ sgn(v(t)) C_i \left(1 - \frac{z_i(t)}{\nu_i s(v(t))}\right) & \text{in sliding mode} \end{cases} \quad (5)$$

$$s(v) = (F_c + (F_s - F_c) e^{-\left(\frac{v}{v_s}\right)^2}) sgn(v) \quad (6)$$

where $s(v)$ is the velocity dependence of the sliding force modeled by a three-parameter function (equation (6)), F_c is the Coulomb force, F_s is the Stribeck force and v_s is the Stribeck velocity. In equation (5), ν_i is a scaling parameter and C_i is the attraction parameter, a gain that determines how fast z_i converges to $\nu_i s(v)$. A GMS element remains in sticking mode until $z_i(t) = \nu_i s(v(t))$ and switches from sliding mode to sticking upon velocity reversal. The output force equation is given as:

$$F_f(t) = \sum_{i=1}^{N} (k_i z_i(t) + \sigma_i \dot{z}_i(t)) + \beta v(t) \quad (7)$$

where $k_i z_i(t)$ represents the elasto-sliding friction force and $\sigma_i \dot{z}_i(t)$ is the viscoelastic behavior.

C. Experimental comparison

In this section an experiment is realized in order to verify if the friction models of the literature can accurately capture the friction phenomena between the seal and the instrument. The results of a velocity step response of a MIS trocar (*AutoSuture* Thoracoport 10.5mm*) equipped with a one stage sealing mechanism is showed on figure 3. In the presliding regime, the reversal of the seal is not modeled by "classical" friction models. The static friction models (Coulomb or Stribeck) are accurate for steady state behavior but they do not capture the deformation mode of the sealing mechanism.

In [5], it has been noticed that four GMS elements are enough to capture the friction force transient under the microscopic deformation assumption. Due to the seal reversal, two "classical" friction transients are observed on figure 3 ($T1$ and $T2$). In order to produce the same pattern as the experimental results, a GMS model requires two times four elements for each transient $T1$ and $T2$ but also at least one element for the transition between these two transients. In order to capture the slope variation occurring at time $0.35s$, one more element is required leading to a total of ten GMS elements. Since three parameters (k_i, σ_i, ν_i) defined the dynamic of the GMS model, this trocar would require 30 parameters plus the $s(v)$ function.

III. Model derivation

As seen in the previous section, the reversal of the seal cannot be described by a GMS model unless a large number of GMS elements (about 10) is used, resulting in a large number of parameters. In this article we propose a new model which can be seen as a Extended Maxwell Slip model (EMS).

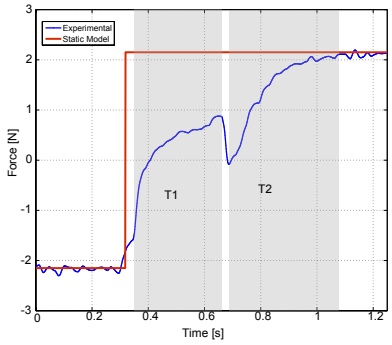

Fig. 3. Friction force measurement upon velocity reversal

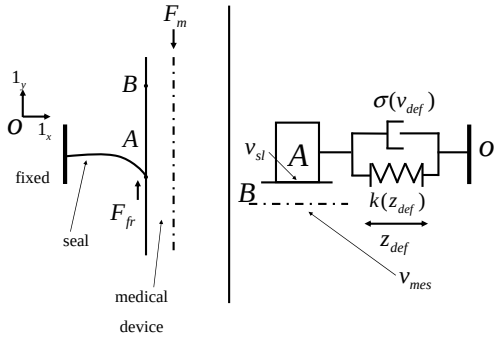

Fig. 4. Schematic drawing of one stage of the trocar sealing mechanism and definition on an EMS elements

A. Physical analysis

Considering an axial symmetry of the medical device and of the seal, the contact between these two bodies can be depicted by the left part of figure 4. During the motion of the medical device, two situations can appear. First, the seal may stick to the medical device. Secondly, the medical device may slide on the seal. These two situations lead to the two operating modes of an EMS element, the deformation mode which replaces the sticking mode of the GMS model, and the sliding mode. In the deformation mode the friction force F_f corresponds to the force required to deform the seal. In sliding mode the friction force corresponds to the sliding force between the seal and the instrument.

In figure 4, O is a fixed reference, A is the contact point between the medical device and the seal of the trocar and B an arbitrary fixed point on the medical device. An EMS element is defined by the right part of figure 4 and is characterized by three variables, the spring deformation amplitude z_{def}, the spring deformation velocity $\dot{z}_{def}$ and the relative velocity between the instrument and the seal v_{sl}. The medical device velocity v_d does not correspond to the sliding velocity v_{sl}. In fact, figure 4 clearly shows that:

$$v_d = \dot{z}_{def} + v_{sl} \tag{8}$$

The deformation force F_{def} is assumed to be modeled by a spring and a damper. This force is computed by :

$$F_{def} = k(z_{def})z_{def} + \sigma(\dot{z}_{def})\dot{z}_{def} \tag{9}$$

The variable stiffness of the spring is modeled by a function of the amplitude of deformation only $k(z_{def})$. The viscoelastic part is modeled by a damping function $\sigma(\dot{z}_{def})$ which depends only on the deformation velocity.

B. Model derivation

The input of the model is the velocity of the medical device and the output is the friction force between the medical device and the seal. For each operating mode the dynamics of the model are related to the variation of the spring deflection.

1) ***In deformation mode:*** it is assumed that the sliding velocity is equal to zero ($v_{sl} = 0$). Hence, equation (8) becomes $v_d = \dot{z}_{def}$. Since the friction force corresponds to the deformation force $F_f = F_{def}$, and substituting $v_d = \dot{z}_{def}$ in (9), the model becomes:

$$\begin{cases} \dot{z}_{def} &= v_d \\ F_f &= k(z_{def})z_{def} + \sigma(v_d)v_d \end{cases} \tag{10}$$

An EMS elements remains in deformation mode till the deformation force is greater than the sliding force. The sliding force is computed by a static friction model like the Stribeck model:

$$\begin{aligned} F_{sl}(v_{sl}) &= (F_c + (F_s - F_c)e^{-\left(\frac{v_{sl}}{v_s}\right)^2})sgn(v_{sl}) + \beta v_{sl} \\ &\triangleq g(v_{sl})sgn(v_{sl}) + \beta v_{sl} \end{aligned} \tag{11}$$

Since there is no sliding ($v_{sl} = 0$), the switching event occurs when:

$$F_f = F_s sgn(v_d) \tag{12}$$

In this equation, $sgn(v_d)$ replaces the undefined $sgn(v_{sl})$.

2) ***In sliding mode:*** the dynamic equation is found by assuming that the force maintaining the spring deformed is equal to the sliding force:

$$k(z_{def})z_{def} + \sigma(\dot{z}_{def})\dot{z}_{def} = F_{sl}(v_{sl}) \tag{13}$$

By substituting equation (11) for $F_{sl}(v_{sl})$ in (13) and by using expression $v_{sl} = v_d - \dot{z}_{def}$, the implicit state equation of model (14) is obtained. Since, by hypothesis, the friction force corresponds to the sliding force $F_f = F_{sl}$, and the deformation force is equal to the sliding force (equation (13)), the output equation of the model remains unchange, and the model becomes:

$$\begin{cases} \dot{z}_{def} &= \frac{g(v_d - \dot{z}_{def})sgn(v_d) + \beta v_d - k(z_{def})z_{def}}{\sigma(\dot{z}_{def}) + \beta} \\ F_f &= k(z_{def})z_{def} + \sigma(\dot{z}_{def})\dot{z}_{def} \end{cases} \tag{14}$$

In the dynamical equation , $sgn(v_{sl})$ is replaced by $sgn(v_d)$. This assumption means that, in sliding mode, the seal may deform in the opposite direction of the medical device or in the same direction but at a slower velocity than the medical device. Indeed, if $sgn(v_{sl}) \neq sgn(\dot{z}_{def})$, then $sgn(v_{sl}) = sgn(v_d)$ and if $sgn(v_{sl}) = sgn(\dot{z}_{def})$, then $sgn(v_{sl}) = sgn(v_d)$ when $|\dot{z}_{def}| < |v_d|$. The switching events from the sliding mode to the sticking mode occurs upon a reversal of the device velocity.

C. Model properties and stability analysis

In this section some properties of the model presented in the previous section are explained. Since the velocity of the device is the input of the model, this velocity is referred below as the input velocity. the main hypothesis concerns the value of $\partial k(z_{def})z_{def}/\partial z_{def}$. This value is negative only when the seal reverses.

Proposition III.1 Steady state mode

Let the input velocity v_d be a constant V. If

$$\begin{cases} \partial k(z_{def})z_{def}/\partial z_{def} \leq 0 & \text{for } z_{def} \in [z_{def}^{min}, z_{def}^{max}] \\ \partial k(z_{def})z_{def}/\partial z_{def} > 0 & \text{elsewhere} \end{cases} \quad (15)$$

then, as $t \to \infty$, all the EMS elements will reach the sliding mode.

Proof: If, at the instant t_0, the EMS elements are in sliding mode then, if the input velocity is constant, by definition the elements will remain in this mode $\forall t \geq t_0$.

If, at the instant t_0, some EMS elements are in deformation mode then after a finite time these elements will reach the sliding mode. In fact, if the input velocity is constant positive (respectively negative) and if the model is in the deformation mode, according to equation (10), the deformation amplitude z_{def} will increase (respectively decrease). When $z_{def} \geq z_{def}^{max}$ (respectively $z_{def} \leq z_{def}^{min}$), F_f will increase (respectively decrease) till equation (12) is fulfilled, showing that the steady state mode of an EMS element is the sliding mode. ■

Proposition III.2 Steady state behavior

Let the input velocity v_d be a constant V and assume that all the EMS elements are in the sliding mode. Then, at steady state, the friction force is computed by

$$F_f^{ss} = g(V)sgn(V) + \beta V \quad (16)$$

and the deformation amplitude by

$$k(z_{def}^{ss})z_{def}^{ss} = g(V)sgn(V) + \beta V \quad (17)$$

Proof: Since the steady state is defined by $\dot{z}_{def} = 0$, equation (8) becomes $v_{sl} = V$. Since, in sliding mode the output force is, by definition, equal to the sliding force, the substitution of the previous relation in equation (11) leads directly to (16) and the substitution of the same relation in equation (13) leads to equation (17). ■

The stability of the steady state behavior is not obvious since equation (14) is not an explicit characterization of the evolution of the state z_{def}. In the particular case considered below in section IV, the functions $\sigma(\dot{z}_{def})$ and $g(v_{sl})$ are constant. In this special case, the stability of the steady state is easily shown by Lyapunov's indirect method. The following result also holds if $g(v_{sl})$ corresponds to a Stribeck model. However this proposition is not proved here.

Proposition III.3 Steady state stability

Let the input velocity v_d be a constant V and let the functions $\sigma(\dot{z}_{def})$ and $g(v_{sl})$ be constant defined as follow,

$$\sigma(\dot{z}_{def}) = \sigma \quad , \quad g(v_{sl}) = F_c \quad (18)$$

If

$$\left(\partial k(z_{def})z_{def}/\partial z_{def}\right)(z_{def}^{ss}) > 0 \quad (19)$$

Then, as $t \to \infty$, the steady state ($z_{def} = z_{def}^{ss}$) is stable.

Proof: The stability of the steady state is analyzed using the Lyapunov's indirect method. The substitution of assumptions (18) in equation (14) leads to

$$\begin{aligned} \dot{z}_{def} &= \frac{F_c sgn(v_d) + \beta v_d - k(z_{def})z_{def}}{\sigma + \beta} \\ &\triangleq f(z_{def}, v_d) \end{aligned} \quad (20)$$

The linearization of the dynamic around the steady state $z_{def} = z_{def}^{ss}$ is characterized by:

$$A_{sl}(z_{def}^{ss}) \triangleq \frac{\partial f(z_{def}, v_d)}{\partial z_{def}}(z_{def}^{ss}, V) \quad (21)$$

where $A_{sl}(z_{def}^{ss})$ is a scalar. Lyapunov's indirect method guaranties than if the scalar A_{sl} exists and if A_{sl} is negative, then the system will be locally exponentially stable around this steady state [6]. The computation of the linearization of (20) around (z_{def}^{ss}) is given by:

$$A_{sl} = -\frac{\partial (k(z_{def})z_{def})}{\partial z_{def}}(z_{def}^{ss})/\left(\sigma + \beta\right) \quad (22)$$

Since σ and β are positive constant, A_{sl} is negative and the system described by equation (20) is stable if equation (19) is fulfilled. ■

IV. Identification

The model of an *AutoSuture* Thoracoport 10.5mm* trocar has been identified. This trocar is a one stage sealing mechanism. The schematic of the experimental setup is depicted in figure 5. A linear motor (*LinMot Stator PS01-23x80-R, Slider PL01-12x350/300 and Guide LM01-23x80/260*) is connected to a medical device simulated by a PVC rods (*diameter = 10 mm*). The motor is capable of $260mm$ stroke limited for safety reason to $160mm$. An internal encoder measures the position with $4\mu m$ resolution. The connection between the motor and the medical device is instrumented by a force sensor of $22N$ capacity (*Futek FSH01553*) in order to measure the friction force in the trocar. The whole system is placed vertically in order to reduce the impact of the gravity on the seal.

An EMS elements is characterized by three functions. $k(z_{def})$ represents the elastic deformation of the seal, $\sigma(\dot{z}_{def})$ is the visco-elastic deformation part and $g(v_{sl})$ corresponds to the sliding force. The identification approach is composed of two step. The first step is the identification of the steady state behavior described by equation (16) (see proposition III.2). The second step is the identification of the two functions $k(z_{def})$ and $\sigma(\dot{z}_{def})$

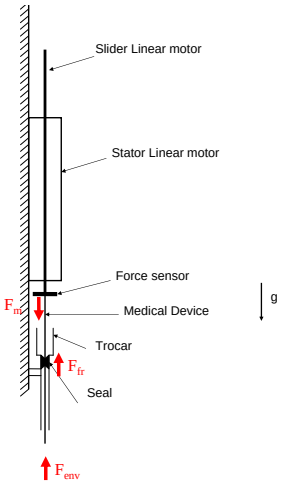

Fig. 5. Schematic of the experimental setup

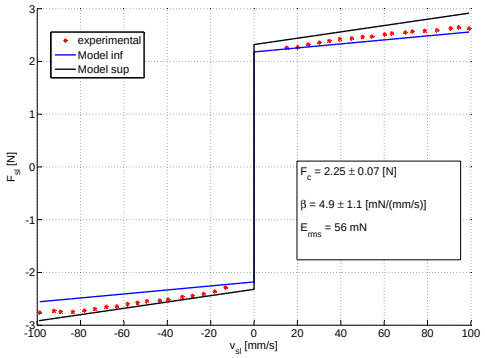

Fig. 6. Static friction force of an *AutoSuture* Thoracoport 10.5mm* trocar

A. Steady state behavior identification

Since the steady state behavior of the model is entirely characterized by (16), and since all the variables of (16) can be measured, the parameters of $g(v_{sl})$ and β are estimated first. The identification of the steady state behavior requires a motion at constant velocity of the medical device. This is achieved by using a PI controller to control the speed of the linear motor. After the friction force reaches its steady state, the velocity and the force are measured.

The experiment consist in performing cyclic upward and downward movements of the instrument through the trocar, with the most significant part of the motion at constant velocity. After each cycle the velocity is incremented by $5mm/s$. The total range of velocity is $\pm 15mm/s$ to $\pm 100mm/s$.

The static friction curve, namely the friction force at steady state versus the sliding velocity, is shown in figure 6. The experimental data are depicted by red stars. The Coulombian characteristic of the friction force is clearly noticed. The static friction model described by (23) is identified by minimizing a least square cost criterion.

$$F_{sl} = F_c sgn(v_{sl}) + \beta v_{sl} \tag{23}$$

The result of the identification of the function F_f^{ss} is depicted in figure 6. The 95% confidence interval for each parameter is also shown. The blue line corresponds to the model with the lowest values for the parameters F_c and β and the black line corresponds to the model with the highest values. For each sign of the sliding velocity, figure 6 shows that the friction force is symetric with respect to the direction of the movement.

B. Dynamic behavior identification

The functions $k(z_{def})$ and $\sigma(\dot{z}_{def})$ are identified in a second step. After the identification of the parameter $F_s = F_c$, the switching surface described by equation (12) is known. Using this knowledge, it is possible to determine all the measurements points $v_d(t_i), F_f(t_i)\ t_i \in [t_0, t_0 + k\Delta t]$ that corresponds to the deformation mode in the upward or downward direction. Equation (10) then yields after discretization

$$\begin{cases} z_{def}^u(t_i) = \sum_{k=0}^{i} v_d(t_0 + k\Delta t)\Delta t + z_{def}^u(t_0) \\ z_{def}^d(t_i) = \sum_{k=0}^{i} v_d(t_0 + k\Delta t)\Delta t + z_{def}^d(t_0) \end{cases} \tag{24}$$

Where z_{def}^u corresponds to the deformation amplitude during upward motion and z_{def}^d during downward motion. Letting t_0 the switching time from the sliding mode to the deformation and $t_0 + N\Delta t$ corresponds to the last time at which condition (12) is fulfilled during the cyclic upward/downward movement, one deduces that $z_{def}^{u/d}(t_0) - z_{def}^{u/d}(t_0 + N\Delta t)$ is the maximum deformation amplitude of the seal in the deformation region. Setting $z_{def}^{u/d}(t_0) - z_{def}^{u/d}(t_0 + N\Delta t) = 2c$, one chooses $z_{def}^{u/d}(t_0)$ in such a way that $z_{def} \in [-c, c]$ for all data samples.

The evolution of the seal deformation has been rebuilt with the data obtained during the steady state experiment. For a certain deformation amplitude (e.g. $z_{def} = 5mm$) the friction force is measured for each value of the deformation velocity. In fact, in deformation mode, the deformation velocity is equal to the velocity of the instrument. Figure 7 depicts the friction force when the deformation amplitude $z_{def} = 5mm$ in function of the deformation velocity. The gray rectangles correspond to the force error due to an error on z_{def} of $0.35mm$. No significant influence of the deformation velocity is observed. Hence $\sigma(\dot{z}_{def})$ is assumed to be equal to zero. The deformation force is then only modeled by a function of the deformation amplitude $F_{def} = k(z_{def})z_{def}$.

For the identification of $F_{def} = k(z_{def})z_{def}$, the experiment consists in performing five cycles of insertion/taking out of the instrument with a constant input force. The deformation amplitude is rebuild using the same method as above. The dependency of the deformation force versus the amplitude of the deformation is plotted in blue in figure 8.

For each phase of the deformation ($v_{def} > 0$ and $v_{def} < 0$) the deformation force is characterized by the following model (equation (25)), where the switch from one polynomial to the other corresponds to the seal reversal.

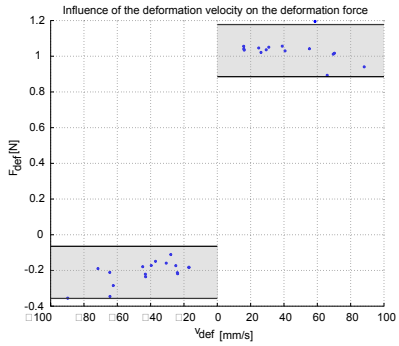

Fig. 7. Influence of the deformation velocity $\dot{z}_{def}$ on the deformation force F_{def}

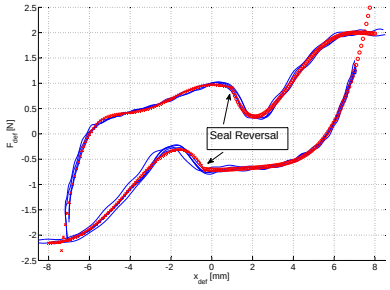

Fig. 8. Identified deformation force of an *AutoSuture* Thoracoport 10.5mm* trocar

$$\hat{F}_{def}(k) = \begin{cases} \sum_{i=0}^{n_1} \theta_i^1 z_{def}^i(k) & \text{if } z_{def}(k) < a \\ \sum_{i=0}^{n_2} \theta_i^2 z_{def}^i(k) & \text{else} \end{cases} \quad (25)$$

This model requires the estimation of the parameters $\theta = [\theta_0^1, \ldots, \theta_{n_1}^1, \theta_0^2, \ldots, \theta_{n_1}^2]$ and a. The constant a is chosen such that : $\sum_{i=0}^{n_2} \theta_i^2 a^i = \sum_{i=0}^{n_1} \theta_i^1 a^i$. The parameter are identified by minimizing the cost function:

$$J_\theta = \sum_{k=0}^{N} \left(\hat{F}_{def}(k) - F_{def}(k) \right)^2 \quad (26)$$

where F_{def} is the part of the friction force measured during the deformation mode.

Figure 8 presents the results of the identification of θ. In this case $n_1 = n_2 = 4$ and the identified polynomial function of degree four are depicted in red. We also compare the model (equation (25)) with a single seven-degrees polynomial. The seven-degrees polynomial has two main drawbacks, firstly the seal reversal is less accurately captured, and secondly some oscillations appear in the neighborhood of $z_{def} = 6mm$.

C. Cross Validation of the EMS model

All the three characteristic functions of the EMS model have been identified. In this section a new set of measurements is used in order to perform a cross validation of the resulting model. The measurements used for the cross validation were obtain by constant velocity motion of the medical device and a stroke of $40mm$. After each cycle the velocity is increased by $5mm/s$. This experiment allows the analysis of the influence of the movement velocity on the accuracy of the model.

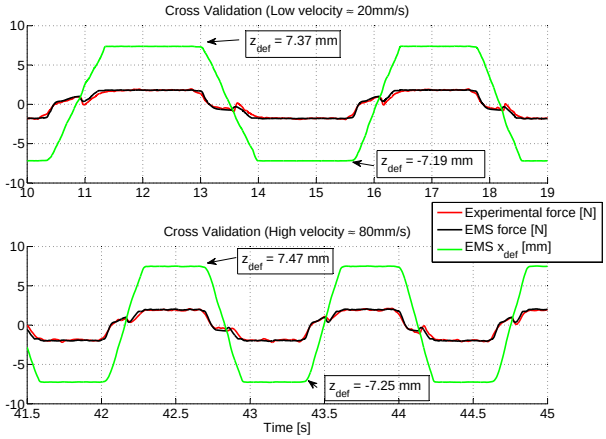

Fig. 9. Comparison between the EMS model and the friction in an *AutoSuture* Thoracoport 10.5mm* trocar

The EMS model responses at high velocity ($80mm/s$) and low velocity ($15mm/s$) are plotted on figure 9. These figures show three variables, the experimental measurements of the friction force, the computed friction force and the computed amplitude of deformation. The global RMS error of the model is about $0.17N$. The EMS model follow the shape of the experimental measurements as well at low velocity then at high velocity. In section IV-B, we assume a common value of the deformation amplitude for the initial condition when the instrument is inserted in the trocar. This assumption is validated in figure 9 but comparing the computed deformation amplitude at high and low velocity.

V. Conclusions

This paper presents and validates a new model for the friction force between the instrument and the trocar used in MIS (*AutoSuture* Thoracoport 10.5mm*).

References

[1] B. Bona and M. Indri, "Friction compensation in robotics: an overview," *IEEE conference on decision and control, and the European control conference, Seville*, 2005.

[2] B. Armstrong, P. Dupont, and C. Canudas De wit, "A survey of models, analysis tools and compensation methods for the control of machines with friction," *Automatica*, vol. 30, no. 7, pp. 1083–1138, 1994.

[3] V. Lampaert, J. Swevers, and F. Al-Bender, "Modification of the leuven integrated friction model structure," *IEEE Transactions on automatic Control*, vol. 47, no. 4, pp. 683–687, 2002.

[4] F. Al-Bender, V. Lampaert, and J. Swevers, "The generalized maxwell-slip model: a novel model for friction simulation and compensation," *IEEE transactions on automatic control*, vol. 50, no. 11, p. 1883:1887, 2005.

[5] T. Tjahjowidodo, F. Al-Bender, H. Van Brussel, and W. Symens, "Friction characterization and compensation in electro-mechanical systems," *Journal of sound and vibration*, 2007. [Online]. Available: http://dx.doi.org/10.1016/j.jsv.2007.03.075

[6] D. Liberzon, *Switching in Systems and Control*. Birkhauser, 2003.